Photochemical & Photobiological Sciences

Accepted Manuscript

ROYAL SOCIETY OF CHEMISTRY

www.rsc.org/pps

Catechin as a new improving agent for photo-Fenton-like system at near-neutral pH for the removal of inderal

Zongping Wang[a], Yizhou Guo[a], Zizheng Liu[*ab], Xiaonan Feng[a], Yiqun Chen[a], Tao Tao[a]

[a]*School of Environmental Science and Engineering, Huazhong University of Science and Technology, Wuhan, 430074,China*

[b]*School of Civil Engineering,Wuhan University, Wuhan, 430074,China*

Abstract

Photodegradation of inderal in a photo-Fenton like system at near-neutral pH modified with catechin, a natural catecholate siderophore, was investigated under simulated sunlight. Main factors influencing the process, such as Fe(III)–catechin complexes, pH, and catechin concentration were examined. Photodegradation of inderal was strongly dependent on pH, following the order pH 3.0 < 5.0 < 7.0 < 6.0. Formation of the Fe(III)-catechin complex resulted in the stabilization of ferric iron and generation of $^{\bullet}OH$ under irradiation at near-neutral pH values. The removal of inderal was about 75% under optimal conditions (50 μmol/L Fe(III) and 200 μmol/L catechin at pH 6.0). Photodegradation products of inderal were identified by LC-ESI-MS and GC-MS, and the photodegradation pathway was proposed. Iron in

[*] Corresponding author. Tel.: +86-27-87792406; Fax: +86-27-87792101.
E-mail address: lzz@hust.edu.cn (Z.Z. Liu).

the Fe(III)–catechin system was reused by simple addition of catechin to the reaction mixture. Results of the present work suggest that the Fe(III)–catechin complex may be used in the photo-Fenton like process, an advanced approach to the removal of organic pollutants at near-neutral pH.

Keywords: Fe(III)–catechin complex; Catecholate siderophore; Photo-Fenton; Neutral pH; Inderal

1. Introduction

Processes based on hydroxyl radical (•OH) chemistry are currently used for the degradation of organic contaminants. Much is known about the nature of the Fenton reaction, which has been widely used as a source of •OH, since its first description in a paper published in 1894 [1]. In recent decades, studies have been done to examine the application of various types of Fenton reactions in wastewater treatment. These reactions include homogeneous Fenton (and Fenton like) processes and photo-Fenton (and photo-Fenton like) systems using various Fe(II) and/or Fe(III) salts and peroxide in acidic media. One system that has been found to be most effective for removal of various organic pollutants from aqueous media, soils, and sediments is the photo-Fenton reaction [2-6], which generates mainly the highly reactive radical •OH [7-9].

However, the traditional Fenton like system has several drawbacks, in particular, its limited pH range and ferric iron precipitation during the process. To overcome these deficiencies, different approaches have been used in related studies. In this regard, one approach that holds promise is the use of organic and inorganic ligands for iron.

Ligands that have been frequently used in photo-Fenton like processes for removal of organic substances in aqueous solutions are citrate [10] and oxalate [11]. Compared with traditional Fenton systems, photo-Fenton-like processes could improve the removal efficiency of substrates by using the aforementioned organic ligands at near−neutral pH. The photo-Fenton like process strongly absorbs ultraviolet–visible (UV–vis) radiation and stabilizes ferric ions over a wider pH range. The high quantum yield of Fe(II) in the presence of ligands increases the amount of $^{\bullet}OH$ generated, thereby increasing the removal efficiency of organic pollutants [12, 13]. Other ligands have also been used to complex iron in photo-Fenton like systems. These include EDTA [14], humic acids [15, 16], and EDDS [17]. Futhermore, Solar photo Fenton was developed to reduce the process time and energy consumption. [18, 19]

Complexes of iron with strong organic ligands comprise >99.9% of dissolved iron in natural environments [20]. This abundance has recently generated much interest in siderophores, iron chelators in biological systems and natural waters as well. Various fungi and heterotrophic bacteria cultured under conditions of limited iron levels have been found to produce siderophores that form complexes with high stability constants [21-24]. The photoreactivity of siderophores is primarily determined by the chemical structure of their Fe(III)-binding groups, namely, hydroxamate and catecholate moieties. Hydroxamate groups are photochemically resistant regardless of Fe(III) complexation. Catecholate siderophores are susceptible to photooxidation and undergo light-induced ligand oxidation and reduction of Fe(III) to Fe(II) [25].

Most of the studies on siderophores were centered on identifying structures [26],

determining dissociation constants for Fe(III)–siderophore complexes [27, 28], and examining iron uptake in the ocean [29]. However, few studies addressed the use of photo-Fenton like systems with Fe(III)–siderophore complexes for remediation of freshwater environments. In the present work, catechin (CAT), which is a natural catecholate siderophores and can be easily obtained from green plants especially Chinese tea, was used as a model catecholate siderophore. We examined the effect of Fe(III)–siderophore complexes on photodegradation of pollutants dissolved in neutral aqueous media. For this purpose, we used inderal, a popular amine drug, as a model pollutant. The effects of Fe(III) complexes, pH values, and catechin concentration on the degradation of inderal in the Fe(III)–catechin system were examined. Generations of $^{\bullet}OH$ and Fe(II) were detected for the photochemical mechanism investigation. Photoproducts of the inderal were determined by LC-ESI-MS and GC–MS, respectively, and the photodegradation pathway was proposed accordingly.

2. Materials and methods

2.1. Materials

Inderal (CAS: 318-98-9, 99%), catechin (CAS: 225937-10-0, 98%), nordihydroguaiaretic acid, pyrocatechol violet, 2,3-dihydroxybenzoic acid, and 2-chloro-3′,4′-dihydroxyacetophenone were purchased from Sigma. Inderal was confirmed from its UV–vis spectra; its molecular structure is shown in Figure A.1. A stock solution of inderal in deionized water was prepared. Ferric chloride (99%) , hydrochloric acid, sodium hydroxide, and benzene were supplied by Wuhan

Chemicals Corporation. All chemicals were of analytical-reagent grade or of higher purity. Doubly distilled deionized water (Milli-Q) was used to prepare all solutions.

2.2. Photolysis experiments

Photolysis experiments were performed in a 60 mL capped cylindrical Pyrex vessel (40 mm i.d., containing 50 mL solution) under a 150 W xenon short-arc lamp. Radiation of wavelengths less than 300 nm was filtered out by using Pyrex glass to simulate sunlight. To measure the quantum yields, the monochromatic irradiations at 300 and 365 nm were carried out with the xenon short-arc lamp equipped with a LOT Oriel grating monochromator. The light and the cells were kept parallel with a fixed distance of 7.0 cm. Lamp output was monitored over time by ferrioxalate actinometry[30] ($Io_{(300\ nm)} \sim = 0.63 \times 10^{14}$ photon $cm^{-2}\ s^{-1}$; $Io_{(365\ nm)} \sim = 1.9 \times 10^{15}$ photon $cm^{-2}\ s^{-1}$). All solutions for the photolysis experiments were freshly prepared prior to irradiation. The pH was measured by using a pHS–3C meter, and adjusted as needed. Aliquots of samples were withdrawn at various intervals, and substrate decay was measured by high-performance liquid chromatography (HPLC).

2.3. Analysis

The concentration of inderal was analyzed on a Shimadzu Essentia LC-15C HPLC system with an Agilent HC-C18 column (5 μm, 250 mm × 4.6 mm). The mobile phase was a solution of acetonitrile and KH_2PO_4 buffer (pH 2.5, 10 mmol/L) at a ratio of 35:65 (v/v). The detector wavelength was 213 nm and the flow rate was 1.0 mL/min. Benzene was used to scavenge $^{\bullet}OH$ in a reaction that produces phenol. The phenol

concentration was analyzed by using a mobile phase of 40:60 (v/v)acetonitrile–H_2O solution, and the detector wavelength was set at 270 nm. The concentrations of ferrous ions were determined using 1,10-phenanathroline spectrophotometry at a wavelength of 510 nm. The concentration of Fe^{3+} was calculated by subtracting the concentration of Fe^{2+} from the total iron concentration in solution. NO_3^- was determined by ion chromatography. The calibration curve for the detection of inderal, $^{\bullet}OH$, and Fe(III) is shown in Figure A.2 (Supplementary Data).

2.4. Photoproduct identification

Photoproducts of inderal were obtained after about 80% of the parent compound had been degraded by Fe(III)–catechin complexes at pH 6.0. The reaction solution was evaporated to dryness in a rotary evaporator. The residue was trimethylsilylated at room temperature with 0.1 mL of hexamethyldisilazane and 0.05 mL of chlorotrimethylsilane. GC–MS was carried out on an Agilent 7890A/5975C system with an HP-5 MS capillary column. The gas chromatograph was operated in temperature-programming mode as follows: hold at initial temperature of 80 °C for 20 min, ramp at 5 °C/min to 280 °C and hold at this temperature for 3 min. The injection port and MSD were held at 250 and 280 °C, respectively.

The LC-MS system used in the study was an Agilent LC/MSD SL ion trap mass spectrometer equipped with an ESI source in the positive ion mode. The mobile phase was (A) 98% H_2O + 2% CH_3CN + 0.2% formic acid and (B) CH_3CN + 0.2% formic acid. Gradient elution was 2% of B for 1 min followed by a linear increase to 95% B at 25 min, and then held constant for an additional 5 min. The mass spectral data were

obtained in the positive ion mode between *m*/*z* 100-300. The settings were: capillary voltage, 3500 V; drying gas, 10 L/min; drying gas temperature, 350°C; capillary exit, 150 V; skimmer, 40 V; octopole RF amplitude, 160Vpp; ICC target, 100 000; trap drive, 60; maximum accumulation time, 100 ms.

3. Results and discussion

3.1. Inderal photodegradation by five Fe(III) complexes

Five kinds of organic ligands were used to complex with Fe(III) at near-neutral pH (6.0) to modify the photo-Fenton like system. The ligands were catechin, nordihydroguaiaretic acid, pyrocatechol violet, 2,3-dihydroxybenzoic acid, and 2-chloro-3′,4′-dihydroxyacetophenone (molecular structures are shown in Table A.1). Inderal degradation through the photo-Fenton like system with various iron complexes was observed Figure 1. The highest efficiency of inderal degradation at pH 6.0 was observed in the photo-Fenton like system with Fe(III)–catechin. About 75% of inderal was removed after 120 min. Degradation of inderal in the presence of Fe(III)–2,3-dihydroxybenzoic acid and Fe(III)–2-chloro-3′,4′-dihydroxyacetophenone complexes in this photo-Fenton like system was negligible (Supplementary Data for nordihydroguaiaretic acid and pyrocatechol violet are shown in Figure A.3). This result may be attributed to the stable complexes that catechin forms with Fe(III) at pH 6.0. By forming such complexes, catechin enhances the solubility and stabilizes Fe(III) in aqueous solution at near-neutral pH (Figure A.4). Thus, catechin has an important contribution to preventing the precipitation of Fe(III) at pH 6.0, and the

Fe(III)–catechin chelate broadens the pH range for iron solubility. These results suggest that catechin may be an effective ligand in the photo-Fenton like system at near-neutral pH.

3.2. Role of CAT and formation of photo-Fenton process

To understand the effect of CAT and irradiation on inderal degradation, experiments using Fe(III)/light (with or without CAT) under the same conditions (50 μmol/L Fe(III) and 200 μmol/L catechin at pH 6.0) were conducted. Results of these experiments (Figure 2) show that direct photodegradation of inderal at near-neutral pH was negligible. When Fe(III) and catechin were used simultaneously without irradiation for 120 min, inderal degradation was negligible. Degradation of inderal in the photo-Fenton like system was faster; ~75% inderal was removed after 120 min. Therefore, irradiation markedly enhanced inderal degradation. This enhancement may be attributed to the photoreactivity of the Fe(III)–catechin complex. The formation of Fe(III)–catechin complex was confirmed by UV–vis spectroscopy of Fe(III), catechin, and Fe(III)–catechin mixture (Figure A.4a). The Fe(III)–catechin mixture produced an obvious spectral shift relative to catechin. There was evidence of formation of a 1:1 ligand–metal complex at near-neutral pH. The conditional stability constant for Fe(III) binding of the Fe(III)–catechin complex was found to be $(1.6 \pm 0.1) \times 10^6$ by continuous variation methods (Figure A.5). Stabilization of Fe(III) at near neutral pH by CAT and formation of photo-Fenton like system are illustrated in Scheme 1. The photo-Fenton like process could be explained by the following reactions [3, 31, 32]:

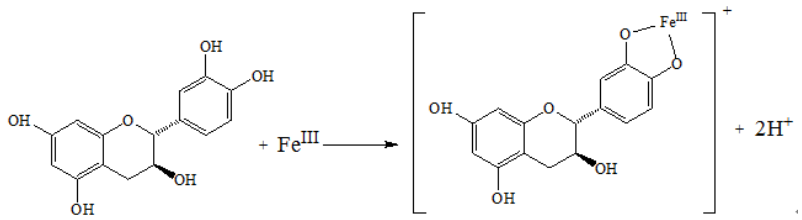

(1)

$$FeCat + h\nu \rightarrow Fe(II) + Cat^{-}\bullet \quad (2)$$

$$Cat^{-}\bullet + O_2 \rightarrow O_2^{\bullet-} \quad (3)$$

$$H^{+} + O_2^{\bullet-} \rightarrow HO_2\bullet \quad (4)$$

$$2HO_2\bullet \rightarrow H_2O_2 + O_2 \quad (5)$$

$$Fe(II)(Cat^{-}) + H_2O_2 \rightarrow Fe(III)Cat + {}^{\bullet}OH + OH^{-} \quad (6)$$

Formation of Fe(III)–catechin complexes evidently increased the rate of $HO_2^{\bullet}/O_2^{\bullet-}$ formation and of $^{\bullet}OH$ formation [33]. These radicals were detected in the reaction solutions (Figure A.6a). During rapid ligand-to-metal charge transfer (LMCT) of the Fe(III)–catechin complex, the species Fe^{2+} and $Cat^{-}\bullet$ are generated. In the presence of oxygen, $O_2^{\bullet-}$ forms and subsequently generates H_2O_2 which, in turn, produces $^{\bullet}OH$ through a reaction with Fe(II) in the Fenton process (Eqs. (3)–(6)). Under acidic conditions, Fe(III) and catechin are free species (Figure A.4b), which have weaker ability to produce $^{\bullet}OH$ compared with the Fe(III)–catechin complex. At near-neutral pH, catechin may increase the solubility and stability of iron. Thus, the Fe(III)–catechin complex becomes a predominant species and has considerable photoreactivity at this pH. On the other hand, the amount of catechin for Fe(III) complexation was more than enough at increased catechin concentration. Thus, it outcompeted hydroxide ions for Fe(III) at higher pH. Therefore, amount of $^{\bullet}OH$ formation increased in the order pH 3.0 < 5.0 < 7.0 < 6.0.

Inderal photodegradation is mainly attributed to the reactive oxygen species, $^{\bullet}$OH. The presence of light played an important role in the production of $^{\bullet}$OH. In the absence of light, $^{\bullet}$OH formation could almost be neglected, in accordance with the comparison between Fe(III)-CAT and photo-Fenton like systems used for inderal degradation. This trend is supported by rate measurements of Fe(III) reduction (Figure A.6b). Results in Figure A.6b show that ~20% of Fe(III) was reduced to Fe(II) at near-neutral pH under irradiation. This result confirms that irradiation affected inderal degradation by enhancing $^{\bullet}$OH generation in the system. Furthermore, the use of irradiation approximating sunlight (main wavelength at 365 nm) makes the process potentially economical and practical.

The effect of the catechin modified photo-Fenton like process on inderal degradation at pH 6.0 was examined to obtain more insight into how $^{\bullet}$OH participates in the process. For this purpose, 2-propanol was used as the scavenger for $^{\bullet}$OH in the solution containing. 50 μmol/L Fe(III), 200 μmol/L catechin, and 10 μmol/L inderal. Results in Figure 3 show that addition of 2-propanol markedly inhibited inderal degradation. 2-Propanol and inderal reacted competitively with $^{\bullet}$OH. Use of 10 mmol/L 2-propanol resulted in removal of only 15% of inderal, demonstrating that inderal degradation was mainly due to the reactivity of $^{\bullet}$OH. When the 2-propanol concentration was increased, the extent of inderal degradation deceased substantially. Thus, these results also indicate that inderal degradation was mainly due to $^{\bullet}$OH.

3.3. Effect of pH

To understand better the optimum pH for the photo-Fenton like process modified

with catechin, experiments at pH 3.0, 5.0, 6.0, and 7.0 were carried out respectively. Initial concentrations of Fe(III), catechin, and inderal were 50, 200, and 10 μmol/L, respectively. The rate of inderal degradation increased in the order pH 3.0 < 5.0 < 7.0 < 6.0 (Figure 4), which is different from the trend for the traditional Fe(III)/light process. The photo-Fenton reaction with Fe(III) was ineffective at pH 3.0 because of chemical equilibrium of Eq. (1) in the solution [31]. Data on $^{\bullet}$OH formation in solutions at various pH values are consistent with this observation (Figure A.6a in Supplementary Data). Therefore, complete complexation of Fe(III) and catechin was essential to the photo-Fenton like system in this work. Under acidic conditions, the chemical equilibrium shifted to the left, leading to the presence of free Fe(III) and catechin. The efficiency of the photo-Fenton like process with Fe(III)-OH complex is quite low compared with that of the process with the Fe(III)–catechin complex. Therefore, the degradation efficiency was low at pH 3.0. The higher efficiency of inderal degradation by the Fe(III)–catechin complex could be attributed to the complexation of iron by catechin, which leads to greater stabilization of iron and formation of hydroperoxyl/superoxide radicals at pH 6.0. We [34] and other investigators [35] also reported similar observations on the photo-Fenton like systems modified with natural or biological products, which are more complicated and not easier to get than catechin.

3.4. Effect of catechin concentration

Inderal photodegradation at pH 6.0 in the presence of catechin at various concentrations was determined. Inderal degradation and catechin concentration were

highly correlated (Figure 5). Use of 50 μmol/L catechin resulted in a degradation rate of <40% over 120 min, whereas addition of 200 μmol/L catechin increased the rate to ~75%. Increasing the catechin concentration from 200 to 500 μmol/L led to a higher rate of inderal removal (from 75% to 85%). This effect is attributed to the high concentration of Fe(III)–catechin complex, which could enhance the formation of $HO_2^{\bullet}/O_2^{\bullet-}$ and $^{\bullet}OH$ and, ultimately, inderal removal. This phenomenon was observed during the degradation of alachlor photoinduced by Fe(III)–citrate complex [10]. On the other hand, when the concentration of catechin is 800 μmol/L, $^{\bullet}OH$ radicals are competitively sequestered by inderal and excess free catechin in aqueous solution; such competition thus decrease the efficiency of inderal degradation.

3.5. Photodegradation products and pathway

Using LC–ESI-MS and GC–MS, we identified products of inderal photodegradation in the catechin modified photo-Fenton system to examine further the mechanism of inderal photodegradation at near-neutral pH. HPLC chromatograms and (+)-ESI-MS spectra of inderal and its photodegradation products after 120 min of photodegradation are presented in Figure A.7. Two products with retention times of 1.4 and 5.0 min were identified. The *m/z* ratio of the photoproduct at 1.4 min is 134 and that of it fragment ion is 92. At 5.0 min, the *m/z* ratio of the photoproduct was 161. $^{\bullet}OH$ attack of side chains ending in their cleavage and oxidation might have led to the formation of this photoproduct.

The low-molecular-weight photoproducts were volatile and detectable by GC–MS. Using the NIST98 library database, we unambiguously identified the main

intermediates of the Fe(III)–catechin system (Table A.2). Mass spectra of standard compounds and photoproducts could be compared in Figure A.8. Table A.2 also indicates that most of the intermediates were hydroxylation products such as 3,4-dihydroxymandelic acid, pyrogallol, protocatechuic acid, *p*-phthalic acid, and gallic acid. $^{\bullet}OH$ may further attack these hydroxylation products, producing a series of low-molecular-weight carboxylic acids. These results thus confirm that inderal photodegradation in the Fe(III)–catechin system mainly involved the reactive oxygen species, $^{\bullet}OH$. As inderal contains an amine group, tests were performed to determine whether inorganic products were formed. NO_3^- and NO_2^- were determined by ion chromatography. Only NO_3^- was detected in the solution. Hence, the amine group of inderal was transformed to inorganic oxy-nitrogen ions. The proposed pathway for inderal photodegradation according to the above results is illustrated in Figure 6. The side chain and benzene ring of inderal first undergo attack by $^{\bullet}OH$, leading to 1,8-dihydroxynaphalene and 1,2-dihydroxy-3-isopropylamino-propane. Subsequent cleavage of one of the benzene rings produces benzene derivatives such as 3,4-dihydroxymandelic acid, pyrogallol, protocatechuic acid, *p*-phthalic acid, and gallic acid. $^{\bullet}OH$ further reacts with the intermediates and generates a series of low-molecular-weight carboxylic acids.

3.6. Reuse of Fe(III)/Fe(II) in solution

In our photo-Fenton like system, the solubility and stability of iron in aqueous solution at near-neutral pH is increased by the use of catechin to form stable complexes with Fe(III). By alternating between the +2 and +3 oxidation states, iron

catalyzes the reaction in the solution. Fe(III)–catechin complexes subjected to irradiation produce Fe(II) via LMCT. As the amount of iron used contributes to the cost of processing and excess amounts discolor the water, a system for Fe(III)/Fe(II) reuse must be in place. In this regard, simple addition of catechin to solutions treated through the photo-Fenton reaction provides a convenient approach.

In our study, three runs were conducted to investigate inderal photodegradation. Initially, the degradation was performed at pH 6.0 with 50 μmol/L Fe(III) and 200 μmol/L catechin. After 120 and 240 min respectively, 200 μmol/L catechin was added to the solution. As shown in Figure 7, the rate constants for inderal photodegradation were 2.3×10^{-4}, 9.5×10^{-5}, and 3.3×10^{-5} s^{-1}, respectively. There was a large effect on inderal removal within 120 min in all three runs. The rate of inderal removal slowly decreased in subsequent runs. Accumulation of intermediates produced during the earlier run may explain this observation. Such intermediates may compete with $^{\bullet}OH$ for reaction with inderal in the solutions.

4. Conclusions

We examined the use of the Fe(III)–catechin complex in the photo-Fenton like process by subjecting inderal-contaminated samples to treatment by the process. The degree and rate of inderal degradation at near-neutral pH was markedly increased upon use of the Fe(III)–catechin complex. By preventing Fe(III) precipitation, catechin contributed to stabilization of Fe(III) at near-neutral pH. Increased efficiency of inderal degradation with increasing pH (3.0 < 5.0 < 7.0 < 6.0) provides evidence

that controlling the pH of the reaction was essential to the efficiency of the process. The efficiency of inderal degradation increased with catechin concentration. The reactive oxygen species $^{\bullet}OH$ was mainly involved in inderal photodegradation in solution. As reuse of iron in the Fe(III)–catechin solution simply involved adding catechin to the reaction solution, recovery of Fe was convenient. Attack of $^{\bullet}OH$ on inderal led to 1,8-dihydroxynaphalene, 1,2-dihydroxy-3-isopropylamino-propane, 3,4-dihydroxymandelic acid, pyrogallol, protocatechuic acid, *p*-phthalic acid, gallic acid, and low-molecular-weight carboxylic acids.

Acknowledgments

This work was supported by a grant from the National Natural Science Foundation of China (51078161, 51409108) and Huazhong University of Science and Technology Independent Innovation Fund (0118261028). Thanks for Huazhong University of Science and Technology Analytical and Testing Center. The anonymous reviewers are also gratefully acknowledged.

Appendix A. Supplementary information

Supplementary information associated with this article can be found in the online version.

References

1. H. J. H. Fenton, LXXIII.—Oxidation of tartaric acid in presence of iron, *J. Chem. Soc., Trans.*, 1894, **65**, 899-910.
2. W. Y. Huang, M. Brigante, F. Wu, C. Mousty, K. Hanna and G. Mailhot, Assessment of the Fe(III)-EDDS complex in Fenton-like processes: from the radical formation to the degradation of bisphenol A, *Environ. Sci. Technol.*, 2013, **47**, 1952-1959.
3. L. Chen, C. Y. Deng, F. Wu and N. S. Deng, Decolorization of the azo dye Orange II in a montmorillonite/H_2O_2 system, *Desalination*, 2011, **281**, 306-311.
4. Y. G. Zuo and J. Zhan, Effects of oxalate on Fe-catalyzed photooxidation of dissolved sulfur dioxide in atmospheric water, *Atmos. Environ.*, 2005, **39**, 27-37.
5. E. M. Glebov, I. P. Pozdnyakov, V. P. Grivin, V. F. Plyusnin, X. Zhang, F. Wu and N.S. Deng, Intermediates in photochemistry of Fe (III) complexes with carboxylic acids in aqueous solutions, *Photoch. Photobio. Sci.*, 2011, **10**, 425-430.
6. Y. Deng and J. D. Englehardt, Treatment of landfill leachate by the Fenton process, *Water Res.*, 2006, **40**, 3683-3694.
7. S. Q. Liu, L. R. Feng, N. Xu, Z. G. Chen and X. M. Wang, Magnetic nickel ferrite as a heterogeneous photo-Fenton catalyst for the degradation of rhodamine B in the presence of oxalic acid, *Chem. Eng. J.*, 2012, **203**, 432-439.
8. L. Y. Ge, H. H. Deng, F. Wu and N. S. Deng, Microalgae-promoted photodegradation of two endocrine disrupters in aqueous solutions, *J. Technol. Biotechnol.*, 2009, **84**, 331-336.

9. A. Durán, J. M. Monteagudo and E. Amores, Solar photo-Fenton degradation of Reactive Blue 4 in a CPC reactor, *Appl. Catal. B: Environ.*, 2008, **80**, 42-50.

10. H. Katsumata, S. Kaneco, T. Suzuki, K. Ohta and Y. Yobiko, Photo-Fenton degradation of alachlor in the presence of citrate solution, *J. Photochem. Photobiol., A*, 2006, **180**, 38-45.

11. Y. Chen, F. Wu, Y. X. Lin, N. S. Deng, N. Bazhin and E. Glebov, Photodegradation of glyphosate in the ferrioxalate system, *J. Hazard. Mater.*, 2007, **148**, 360-365.

12. Y. G. Zuo and J. Hoigné, Evidence for photochemical formation of H_2O_2 and oxidation of SO_2 in authentic fog water, *Science*, 1993, **260**, 71-73.

13. Y. G. Zuo and J. Hoigne, Formation of hydrogen peroxide and depletion of oxalic acid in atmospheric water by photolysis of iron (III)-oxalato complexes, *Environ. Sci. Technol.*, 1992, **26**, 1014-1022.

14. P. Kocot, A. Karocki and Z. Stasicka, Photochemistry of the Fe(III)–EDTA complexes, *J. Photochem. Photobiol., A*, 2006, **179**, 176-183.

15. E. Lipczynska-Kochany and J. Kochany, Effect of humic substances on the Fenton treatment of wastewater at acidic and neutral pH, *Chemosphere*, 2008, **73**, 745-750.

16. C. Fan, L. Tsui and M. Liao, Parathion degradation and its intermediate formation by Fenton process in neutral environment, *Chemosphere*, 2011, **82**, 229-236.

17. W. Y. Huang, M. Brigante, F. Wu, K. Hanna and G. Mailhot, Development of a new homogenous photo-Fenton process using Fe(III)-EDDS complexes, *J.*

Photochem. Photobiol., A, 2012, **239**, 17-23.

18. J. A. Sánchez Pérez, I. M. Román Sánchez, I. Carra, A. Cabrera Reina, J. L. Casas López and S. Malato, Economic evaluation of a combined photo-Fenton/MBR process using pesticides as model pollutant. Factors affecting costs, *J. Hazard. Mater.*, 2013, **244-245**, 195-203.

19. I. Carra, S. Malato, M. Jiménez, M. I. Maldonado and J. A. Sánchez Pérez, Microcontaminant removal by solar photo-Fenton at natural pH run with sequential and continuous iron additions, *Chem. Eng. J.*, 2014, **235**, 132-140.

20. J. Granger and N. M. Price, The importance of siderophores in iron nutrition of heterotrophic marine bacteria, *Limnol. Oceanog.*, 1999, **44**, 541-555.

21. T. P. Murphy, D. R. Lean and C. Nalewajko, Blue-green algae: their excretion of iron-selective chelators enables them to dominate other algae, *Science*, 1976, **192**, 900-902.

22. D. A. Hutchins, A. E. Witter, A. Butler and G. W. Luther, Competition among marine phytoplankton for different chelated iron species, *Nature*, 1999, **400**, 858-861.

23. C. G. Trick, R. J. Andersen, A. Gillam and P. J. Harrison, Prorocentrin: an extracellular siderophore produced by the marine dinoflagellate Prorocentrum minimum, *Science*, 1983, **219**, 306-308.

24. S. A. Amin, D. H. Green, F. C. Küpper and C. J. Carrano, Vibrioferrin, an Unusual Marine Siderophore: Iron Binding, Photochemistry, and Biological Implications, *Inorg. Chem.*, 2009, **48**, 11451-11458.

25. K. Barbeau, E. L. Rue, C. G. Trick, K. W. Bruland and A. Butler, Photochemical

reactivity of siderophores produced by marine heterotrophic bacteria and cyanobacteria based on characteristic Fe (III) binding groups, *Limnol. Oceanog.*, 2003, **48**, 1069-1078.

26. J. D. Martin, Y. Ito, V. V. Homann, M. G. Haygood and A. Butler, Structure and membrane affinity of new amphiphilic siderophores produced by Ochrobactrum sp. SP18, *J. Biol. Inorg. Chem.*, 2006, **11**, 633-641.

27. R. T. Reid, D. H. Livet, D. J. Faulkner and A. Butler, A siderophore from a marine bacterium with an exceptional ferric ion affinity constant, *Nature*, 1993, **366**, 455-458.

28. J. F. Wu and G. W. Luther III, Complexation of Fe (III) by natural organic ligands in the Northwest Atlantic Ocean by a competitive ligand equilibration method and a kinetic approach, *Mar. Chem.*, 1995, **50**, 159-177.

29. S. Pérez-Miranda, N. Cabirol, R. George-Téllez, L. S. Zamudio-Rivera and F. J. Fernández, O-CAS, a fast and universal method for siderophore detection, *J. Microbiol. Meth.*, 2007, **70**, 127-131.

30. C. G. Hatchard and C. A. Parker, A new sensitive chemical actinometer. II. Potassium ferrioxalate as a standard chemical actinometer, *Proc. R. Soc. A*, 1956, **235**, 518-536.

31. M. E. Bodini, M. A. Del Valle, R. Tapia, F. Leighton and L. Gonzalez, Study of the iron catechin complexes in dimethyl sulphoxide. Redox chemistry and interaction with superoxide radical anion in this medium, *Bol. Soc. Chil. Quím.*, 2001, **46**, 309-317.

32. M. J. Hynes and M. Ó Coinceanainn, The kinetics and mechanisms of the reaction of iron (III) with gallic acid, gallic acid methyl ester and catechin, *J. Inorg. Biochem.*, 2001, **85**, 131-142.

33. A. S. Cornish and W. J. Page, The catecholate siderophores of Azotobacter vinelandii: their affinity for iron and role in oxygen stress management, *Microbiology*, 1998, **144**, 1747-1754.

34. Z. P. Wang, Z. Z. Liu, F. Yu, J. P. Zhu, Y. Chen and T. Tao, Siderophore-modified Fenton-like system for the degradation of propranolol in aqueous solutions at near neutral pH values, *Chem. Eng. J.*, 2013, **229**, 177-182.

35. F. Baldi, D. Marchetto, D. Zanchettin, E. Sartorato, S. Paganelli and O. Piccolo, A bio-generated Fe (III)-binding exopolysaccharide used as new catalyst for phenol hydroxylation, *Green Chem.*, 2010, **12**, 1405-1409.

Captions for Figures

Figure 1 − Inderal photodegradation by five Fe(III) complexes. Reaction conditions were as follows: [Fe(III)] = 50 μmol/L, [ligand] = 200 μmol/L, [inderal] =10 μmol/L, pH = 6.0.

Figure 2 − Comparison of Fe(III)/light (with or without CAT) processes. Reaction conditions were as follows: [Fe(III)] = 50 μmol/L, [catechin] = 200 μmol/L, [inderal] = 10 μmol/L, pH = 6.0.

Figure 3 − Effect of 2-propanol on inderal photodegradation. Reaction conditions were as follows: [Fe(III)] = 50 μmol/L, [catechin] = 200 μmol/L, [inderal] = 10 μmol/L, pH = 6.0.

Figure 4 − Effect of pH on inderal photodegradation. Reaction conditions were as follows: [Fe(III)] = 50 μmol/L, [catechin] = 200 μmol/L, [inderal] =10 μmol/L.

Figure 5 − Inderal degradation in the presence of catechins of various concentrations. Reaction conditions were as follows: [Fe(III)] = 50 μmol/L, [inderal] =10 μmol/L, pH = 6.0

Figure 6 − The proposed pathways for indirect photodegradation of inderal in the Fe(III)–catechin system.

Figure 7 − Photodegradation of inderal after addition of catechin (200 μM) to the Fe(III) solution (50 μM) in the three runs at pH 6.0.

Scheme 1 − Stabilization of Fe(III) at near neutral pH by CAT and formation of photo-Fenton system.

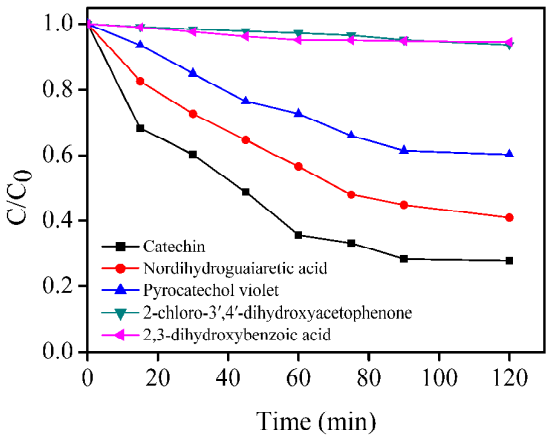

Figure 1 − Inderal photodegradation by five Fe(III) complexes. Reaction conditions were as follows: [Fe(III)] = 50 μmol/L, [ligand] = 200 μmol/L, [inderal] =10 μmol/L, pH = 6.0.

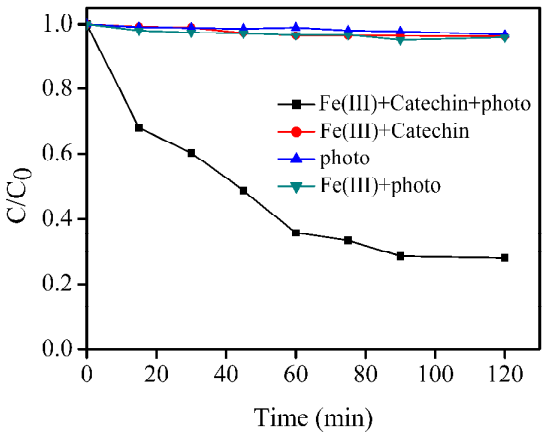

Figure 2 − Comparison of Fe(III)/light (with or without CAT) processes. Reaction conditions were as follows: [Fe(III)] = 50 μmol/L, [catechin] = 200 μmol/L, [inderal] = 10 μmol/L, pH = 6.0.

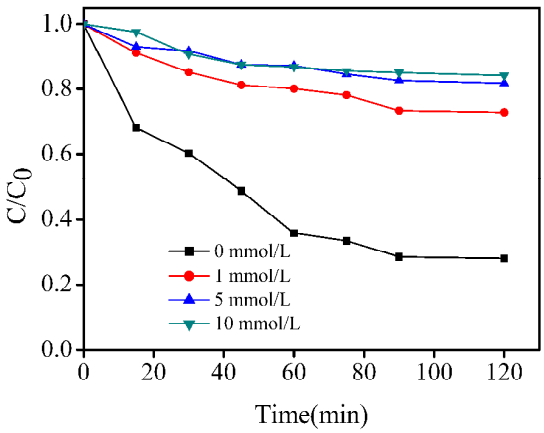

Figure 3 − Effect of 2-propanol on inderal photodegradation. Reaction conditions were as follows: [Fe(III)] = 50 μmol/L, [catechin] = 200 μmol/L, [inderal] = 10 μmol/L, pH = 6.0.

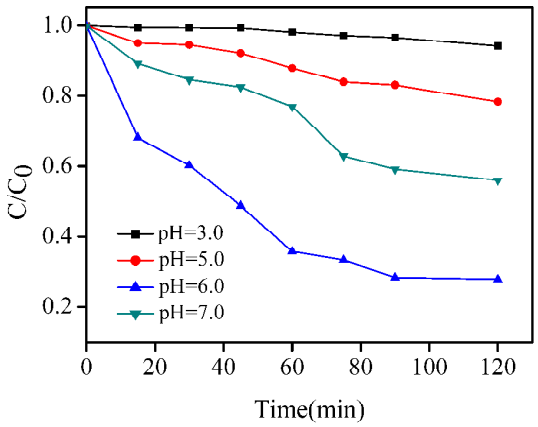

Figure 4 − Effect of pH on inderal photodegradation. Reaction conditions were as follows: [Fe(III)] = 50 μmol/L, [catechin] = 200 μmol/L, [inderal] =10 μmol/L.

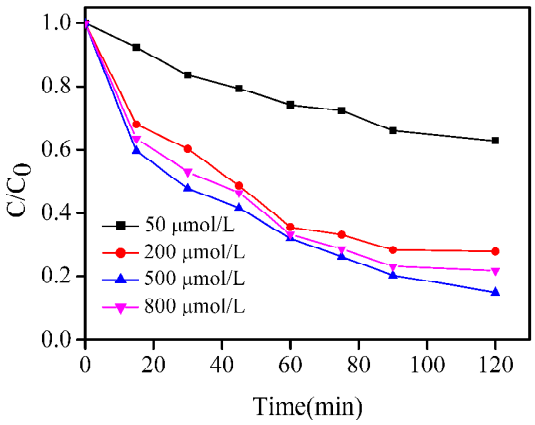

Figure 5 − Inderal degradation in the presence of catechins of various concentrations. Reaction conditions were as follows: [Fe(III)] = 50 μmol/L, [inderal] =10 μmol/L, pH = 6.0

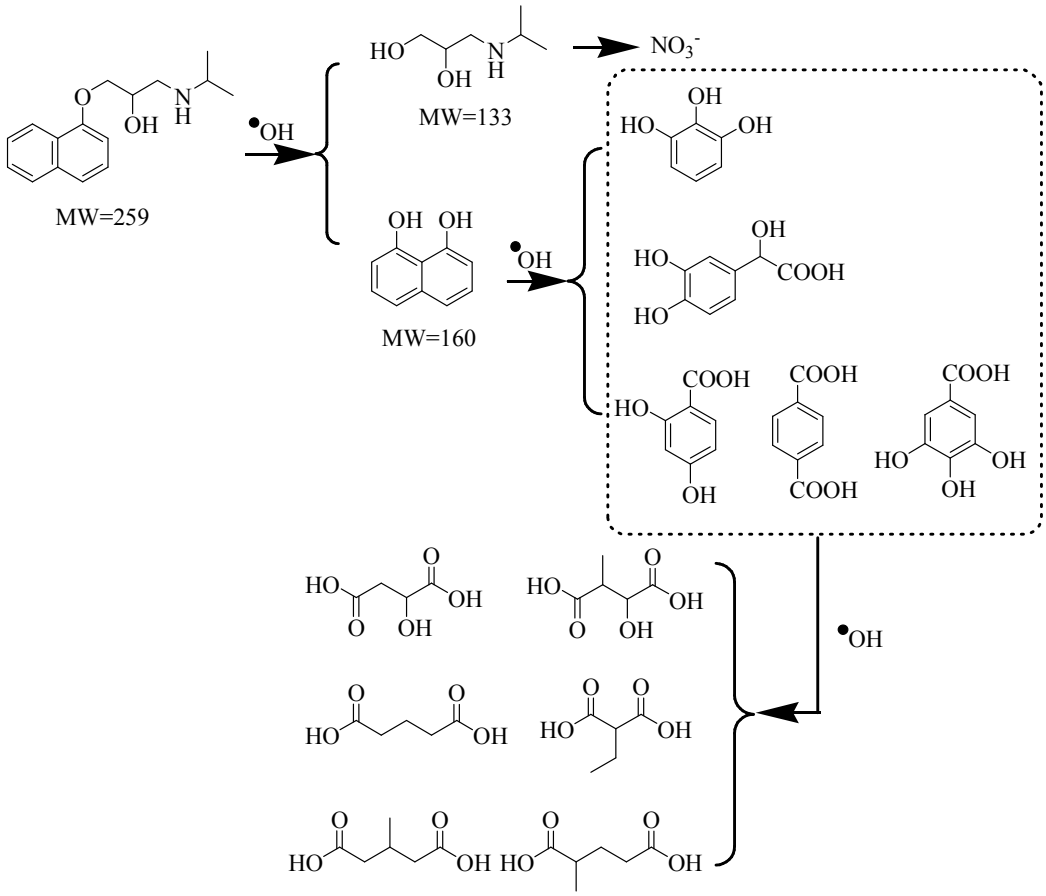

Figure 6 − The proposed pathways for indirect photodegradation of inderal in the Fe(III)–catechin system.

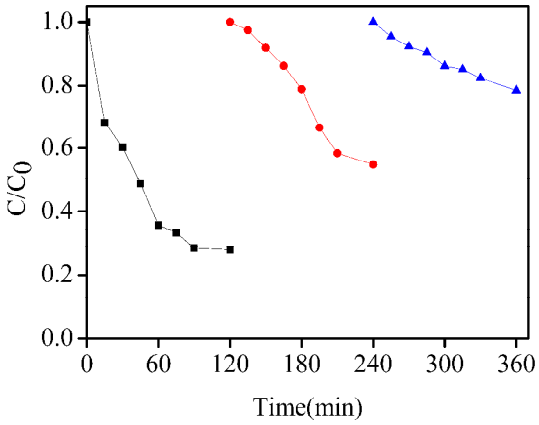

Figure 7 − Photodegradation of inderal after addition of catechin (200 μM) to the Fe(III) solution (50 μM) in the three runs at pH 6.0.

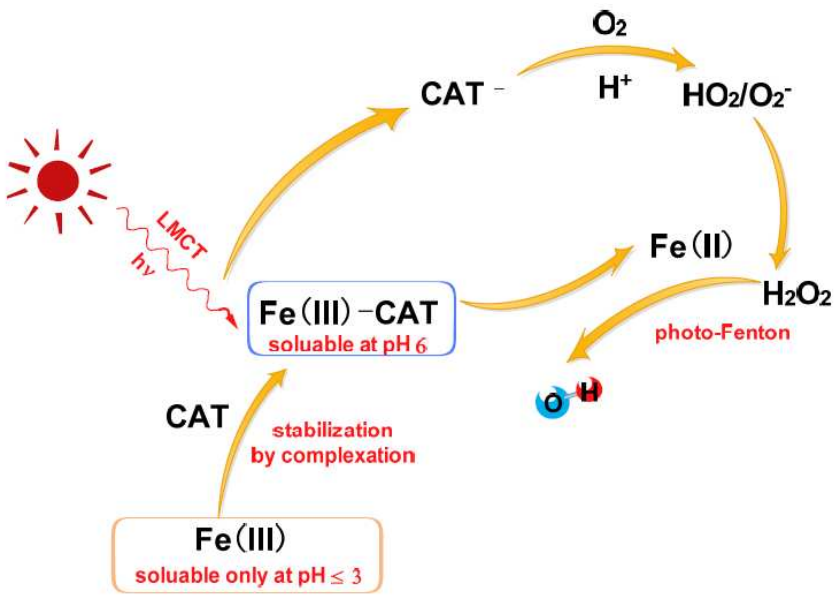

Scheme 1 − Stabilization of Fe(III) at near neutral pH by CAT and formation of photo-Fenton system.